Chemosphere 157 (2016) 10–17

Contents lists available at ScienceDirect

Chemosphere

journal homepage: www.elsevier.com/locate/chemosphere

Metabolic pathways of benzimidazole anthelmintics in harebell (*Campanula rotundifolia*)

Lucie Stuchlíková [a], Robert Jirásko [b], Lenka Skálová [a], František Pavlík [a], Barbora Szotáková [a], Michal Holčapek [b], Tomáš Vaněk [c], Radka Podlipná [c, *]

[a] Department of Biochemical Sciences, Faculty of Pharmacy in Hradec Králové, Charles University in Prague, Heyrovského 1203, 500 05 Hradec Králové, Czech Republic
[b] Department of Analytical Chemistry, Faculty of Chemical Technology, University of Pardubice, Studentská 573, 532 10 Pardubice, Czech Republic
[c] Laboratory of Plant Biotechnologies, Institute of Experimental Botany, Czech Academy of Science, Rozvojová 263, 165 02 Prague, Czech Republic

HIGHLIGHTS

- Benzimidazole anthelmintics albendazole (ABZ), fenbendazole (FBZ) and flubendazole (FLU) were not toxic for harebell cells.
- Harebell cells transformed ABZ, FLU and FBZ into 24, 18 and 29 metabolites, respectively.
- The schemes of metabolic pathways of these anthelmintics were proposed.
- Substantial part of some metabolites could be decomposed to biologically active substances.

ARTICLE INFO

Article history:
Received 11 January 2016
Received in revised form
5 May 2016
Accepted 6 May 2016

Handling Editor: David Volz

Keywords:
Drug metabolism
Biotransformation
Albendazole
Flubendazole
Phytoremediation

ABSTRACT

Benzimidazoles anthelmintics, which enter into environment primarily through excretion in the feces or urine of treated animals, can affect various organisms and disrupt ecosystem balance. The present study was designed to test the phytotoxicity and biotransformation of the three benzimidazole anthelmintics albendazole (ABZ), fenbendazole (FBZ) and flubendazole (FLU) in the harebell (*Campanula rotundifolia*). This meadow plant commonly grows in pastures and comes into contact with anthelmintics through the excrements of treated animals. Suspensions of harebell cells in culture medium were used as an *in vitro* model system. ABZ, FLU and FBZ were not found to be toxic for harebell cells, which were able to metabolize ABZ, FLU and FBZ via the formation of a wide scale of metabolites. Ultrahigh-performance liquid chromatography coupled with high mass accuracy tandem mass spectrometry (UHPLC-MS/MS) led to the identification of 24, 18 and 29 metabolites of ABZ, FLU and FBZ, respectively. Several novel metabolites were identified for the first time. Based on the obtained results, the schemes of the metabolic pathways of these anthelmintics were proposed. Most of these metabolites can be considered deactivation products, but a substantial portion of them may readily be decomposed to biologically active substances which could negatively affect ecosystems.

1. Introduction

Benzimidazoles (e.g. albendazole, ABZ; fenbendazole, FBZ and flubendazole, FLU) represent the most popular class of anthelmintics, the drugs against parasitic worms. Anthelmintics are widely used especially in veterinary medicine for the treatment of various forms of helminthoses. In addition to treatment of diseases, anthelmintics are often used prophylactically in farm animals, which significantly increase the global consumption of these drugs (Harhay et al., 2010) (Sutherland and Leathwick, 2011). According to the annual report of the Institute for State Control of Veterinary Biologicals and Medicines, 1, 244 kg of benzimidazole anthelmintics were sold in Czech Republic in 2014. The efficacy of treatment with anthelmintic drugs is uncontested, however they represent a clear risk to the environment.

Anthelmintics administered to animals enter into the environment primarily through excretion in feces or urine. Following

* Corresponding author. ÚEB AVČR, Rozvojová 263, 165 02 Praha 6, Czech Republic.
E-mail address: podlipna@ueb.cas.cz (R. Podlipná).

http://dx.doi.org/10.1016/j.chemosphere.2016.05.015
0045-6535/

excretion, anthelmintics and their metabolites persist in the environment and may affect various organisms and disrupt terrestrial as well as aquatic ecosystems (Boxall et al., 2003; Boxall and Long, 2005; Floate et al., 2005; Boxall et al., 2012; Arnold et al., 2013). Understandably, free-living helminths along with other invertebrates rank among the most endangered groups of organisms, with several studies having documented the strong negative effects of the anthelmintics on these animals (e.g (Floate et al., 2005; Gao et al., 2007).). Moreover, the exposure of lower development stages of parasitic helminths to low concentrations of anthelmintics in manure and soil may also encourage the development of drug-resistant strains of helminths (Horvat et al., 2012). Ecological hazards of benzimidazole anthelmintics in aquatic ecosystems have been studied with results documenting acute as well as chronic toxicity of ABZ, FBZ and FLU against the freshwater invertebrate *Daphnia magna*, with FBZ being the most toxic (Oh et al., 2006). Also exposure of *Chironomus riparius* larvae to FBZ resulted in a significant toxic effect (Park et al., 2009).

In addition to animals, plants have also been identified as other organisms which may be affected by anthelmintics in the environment. Plants come in contact with anthelmintics and other veterinary drugs in pastures used by treated animals, in fields fertilized with dung from treated animals or in aquatic ecosystems. But in contrast to the situation regarding animals, information about the toxicity and fate of anthelmintics in plants is very limited, despite the fact that this knowledge is vital in the complex evaluation of ecotoxicological impacts.

Anthelmintic which have entered plant cells may be metabolized via the action of biotransformation enzymes. The biotransformation of drugs and other xenobiotics in plants occurs in two phases, with the oxidation, reduction or hydrolysis of the drugs comprising phase I of the process. In this step, reactive and hydrophilic groups are inserted or uncovered in the structures of the xenobiotics. In phase II, xenobiotics or their phase I metabolites can undergo conjugation reactions with endogenous compounds e.g. glutathione, glucose, amino acids; the transport and storage of xenobiotics metabolites in vacuoles or cell walls represent an important part of xenobiotics metabolism (Gonzalez-Mendoza, 2007; Doran, 2009; Verkleij et al., 2009; Cummins et al., 2011). As some drug metabolites can be even more toxic than the parent compound, there is a certain risk that not only parent drugs but also their metabolites could affect plant growth and physiology. Moreover, the consumption of these contaminated plants could affect invertebrates or other animals (Doran, 2009; Verkleij et al., 2009). In spite of this fact, the biotransformation of drugs in plants has only rarely been studied.

To begin to address this lack of information, the present study was designed to test phytotoxicity and biotransformation of the three benzimidazole anthelmintics ABZ, FLU and FBZ in harebell (*Campanula rotundifolia*). This meadow plant grows commonly in pastures and comes into contact with anthelmintics from the excrements of treated animals. Suspensions of harebell cells in culture medium were used as an *in vitro* model system, and the metabolites of anthelmintics were identified using UHPLC-MS/MS. Based on the obtained results, the schemes of ABZ, FBZ and FLU metabolic pathways in harebell were proposed.

2. Materials and methods

2.1. Chemicals and reagents

ABZ and FBZ were purchased from Sigma-Aldrich (St. Louis, MO, USA). FLU was obtained from Janssen Pharmaceutica (New Brunswick, NJ, USA). All other chemicals (UHPLC, MS, or analytical grade) were obtained from Sigma Aldrich (St. Louis, MO, USA).

2.2. Plant cell cultivation

The harebell seeds (*Campanula rotundifolia*) were provided by the Botanical Institute in Průhonice (Czech Republic). The seeds were cleaned in 70% ethanol for 1 min and sterilized by 1% sodium hypochlorite for a period of 10 min. After this they were rinsed 3 times in sterile water and grown on hormone-free solid MS medium (Murashige and Skoog, 1962) with 30 g L^{-1} sucrose, with the germination beginning after 7 days. Callus culture was achieved from primary callus rising on the cut blade and petiole segments of harebell seedlings after replanting them in solid MS medium supplemented by 2,4 -dichlorophenoxyacetic acid and kinetin in concentration (0.225 mg L^{-1}) and (0.215 mg L^{-1}) resp., used previously for callus induction of another species. Suspension cultures derived from this callus were grown in the dark at 24 °C on a rotary shaker at 100 rpm in 250 mL flasks containing 100 mL MS medium supplemented with identical growth regulators. The suspension culture was subcultured at 2-week interval (Podlipna et al., 2015).

2.3. Phytotoxicity assay

The suspension cultures were incubated in MS medium with 10 μM ABZ, FLU or FBZ (pre-dissolved in DMSO) for 1, 4 and 10 days under the conditions described above, with the suspensions supplemented with DMSO without drugs representing the controls. After incubation, the suspensions were filtered using a Bűchnner funnel, with 1 gram of the cells placed into test tubes with 0.8% 2,3,5-triphenyltetrazoliumchloride (TTC) solution in phosphate buffer and left in the dark for 6 h. The rest of the cells were dried and the dry matters weighed; the viable cells produced red formazan via the oxidation of TTC. The cells were filtered again and put into tubes with ethanol; the absorbance of the extracted formazan was measured at 485 nm (Podlipna et al., 2008).

2.4. Incubation of cells with benzimidazole anthelmintics

Ten grams of aseptically filtered cell mass was inoculated into 100 ml of fresh medium in each flask. After 5 days of growth, the medium was supplemented with benzimidazole anthelmintic (ABZ, FLU, FBZ). Prior the addition to the medium, the tested anthelmintics were pre-dissolved in a small amount of DMSO. The final concentration of anthelmintics in medium was 10 μM. The samples (in triplicates) were collected after 24-h incubation, after which the cell suspensions were filtered; the cells were repeatedly washed, transferred into tubes and lyophilized. In the chemical blank samples, medium containing the anthelmintics but not the cell suspension was incubated. In the biological blank samples, the cell suspensions were incubated in a drug-free medium.

2.5. Sample preparation and extraction for analysis

The cell suspensions were homogenized using the FastPrep-24 homogenizer (Santa Ana, CA, USA); homogenized cell suspensions were subjected to liquid-liquid extraction (LLE) according to the method described previously by Vokřál et al. (2012) and Podlipna et al. (2013). The obtained supernatants were evaporated to dryness using the concentrator Eppendorf (30 °C). Dry samples were quantitatively reconstituted in a mixture of acetonitrile/water (70/30, v/v) by sonication and filtrated through syringe filters with GHP membrane. Two microliters of samples were injected into the UHPLC-MS system.

2.6. UHPLC-MS/MS conditions for untargeted analysis

The samples were analyzed using UHPLC-MS/MS with

electrospray ionization (ESI) on a hybrid quadrupole-time-of-flight mass analyzer (micrOTOF-Q, Bruker Daltonics, Germany). UHPLC was performed on an Agilent 1290 Infinity liquid chromatograph (Agilent Technologies, Waldbronn, Germany) using a Kinetex Luna C18 column 150 × 2.1 mm, 1.7 μm (Phenomenex, Torrance, CA, USA), temperature 40 °C, flow rate 0.4 ml/min and the injection volume 2 μl. The mobile phase consisted of water (A) and acetonitrile (B), both with the addition of 0.1% formic acid. The linear gradient was as follows: 0 min–15% B, 8 min–40% B, 10 min–95% B followed by 1 min of isocratic elution. The washing and reconditioning of the column were carried out after linear gradient for all separations. The QqTOF mass spectrometer with average resolving power higher than 13,000 was used with the following setting of tuning parameters: capillary voltage 4.5 kV, drying temperature 220 °C, the flow rate and pressure of nitrogen were 8 l/min and 1.3 bar, respectively. The external calibration was performed with sodium formate clusters before individual measurements. ESI mass spectra were recorded in the range of *m/z* 50–1000 in the positive-ion mode. The isolation width Δ*m/z* 2 and the collision energy 20 eV (found as optimal energy for fragmentation of studied metabolite ions) using argon as the collision gas were employed for MS/MS experiments.

2.7. UHPLC/MS conditions for targeted analysis

A Nexera UHPLC system coupled with a LCMS-8030 triple quadrupole mass detector (both from Shimadzu, Japan) operating in ESI positive mode was used for the targeted analysis of the main metabolites of anthelmintics formed by harebell cells. The acquired data were processed using LabSolutions software (v. 5.60 SP2, 2013, Shimadzu, Japan). UHPLC was performed using a Zorbax RRHD Eclipse Plus C18 column 150 × 2.1 mm, 1.8 μm (Agilent Technologies, Waldbronn, Germany), temperature 40 °C, flow rate 0.4 ml/min and injection volume 1 μl. The mobile phase and linear gradient were the same as previous qualitative analyses. MS was used with the following settings of tuning parameters: capillary voltage 4.5 kV, heat block temperature 400 °C, DL line temperature 250 °C, and flow rate of nitrogen 12 l/min. Argon was used as collision gas. The relative peak areas of the metabolites were integrated using the internal standard mebendazole (MBZ). Values were expressed as percentages, with the sum of relative peak areas for individual anthelmintics representing 100%.

2.8. Statistical analysis

Data analysis was performed using 2way ANOVA with a Bonferroni post hoc test (comparisons of multiple groups against a corresponding control) (GraphPad Prism Software, La Jolla, CA, USA). All values were expressed as mean ± SD. A probability of $p < 0.05$ was considered statistically significant.

3. Results

3.1. Test of the potential phytotoxicity of benzimidazole anthelmintics

Incubation of the harebell cells with the benzimidazole anthelmintics ABZ, FLU and FBZ (at concentrations 10 μM) for 1, 4 and 10 days did not significantly affect the growth and viability of cell suspensions (see Fig. 1).

3.2. Biotransformation of benzimidazole anthelmintics in harebell cells

The biotransformation of ABZ, FLU and FBZ was studied in harebell cell suspensions. Suspension cultures were grown in medium supplemented with ABZ, FLU and FBZ for 24 h. After incubation, samples of cells were collected, extracted and consequently analyzed using UHPLC-MS/MS.

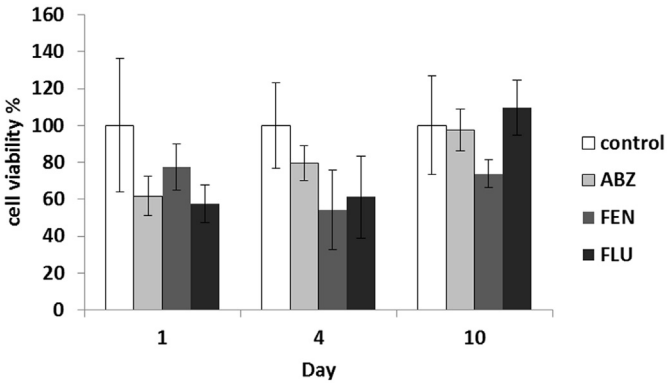

Fig. 1. The effect of benzimidazole anthelmintics (10 μM) on harebell cell viability after 1-, 4- and 10-day incubations. The data expressed in percentages represent the mean ± S.D. of untreated controls (=100%).

All measurements were carried out in the positive-ion mode for increased sensitivity. Detected metabolites were identified based on the presence of protonated molecules $[M+H]^+$ and the interpretation of their product ion spectra. In some cases, the position of the hydroxyl and methyl group nor the position of glucose conjugation or *O*-acetylglucoside conjugation could be determined on the basis of the fragmentation ions, see Figs. 2–4.

High mass accuracy measurement allows the confirmation of elemental composition and the types of metabolic reactions according to exact mass defects (Holčapek et al., 2008). The obtained experimental values of $[M+H]^+$ differ from the theoretical values by less than 4 ppm calculated according to the definition of mass accuracy. Retention times, theoretical *m/z* values of elemental composition, product ions of metabolites and concentration of metabolites after 24 h of FLU, ABZ and FBZ are summarized in Tables 1–3, respectively.

3.2.1. Flubendazole

Three type of reactions were identified as FLU phase I biotransformation: carbonyl reduction, hydroxylation or epoxidation and hydrolysis. FLU with reduced carbonyl groups ($M9_{FLU}$) represented the main FLU metabolite phase I biotransformation. Additional FLU metabolite was formed via arene hydroxylation ($M15_{FLU}$, $M16_{FLU}$). These I metabolites of FLU possessed the characteristic neutral loss (NL) of methanol Δ*m/z* 32. Hydrolysis of the peptide bond in the FLU structure led to the formation of FLU metabolites without a side chain.

Regarding phase II of FLU biotransformation, conjugation with UDP-glucose predominated. The parent FLU as well as FLU metabolites formed via phase I biotransformation underwent *N*-glucosidation, leading to formation of $M11_{FLU}$, $M13_{FLU}$ (the main FLU metabolite of phase II biotransformation), $M17_{FLU}$, $M1_{FLU}$, $M5_{FLU}$ and $M18_{FLU}$. The NLs of Δ*m/z* 162, characteristic for glucose, and Δ*m/z* 32, characteristic for methanol (with the exception of hydrolysed metabolites), were observed in tandem mass spectra of all these conjugates. $M9_{FLU}$ was conjugated with glucose in two ways, *N*-glucosidation ($M11_{FLU}$, $M13_{FLU}$ and $M17_{FLU}$) and/or *O*-glucosidation ($M2_{FLU}$ and $M3_{FLU}$). The different position of glucose conjugations is recognized based on typical NL Δ*m/z* 162 of glucose for *N*-glucosides, and Δ*m/z* 162 of glucose plus Δ*m/z* 18 of H_2O for *N*- or *O*-glucosides. Methylation represented the second type of $M9_{FLU}$ conjugation as its methyl-derivative ($M12_{FLU}$) was found.

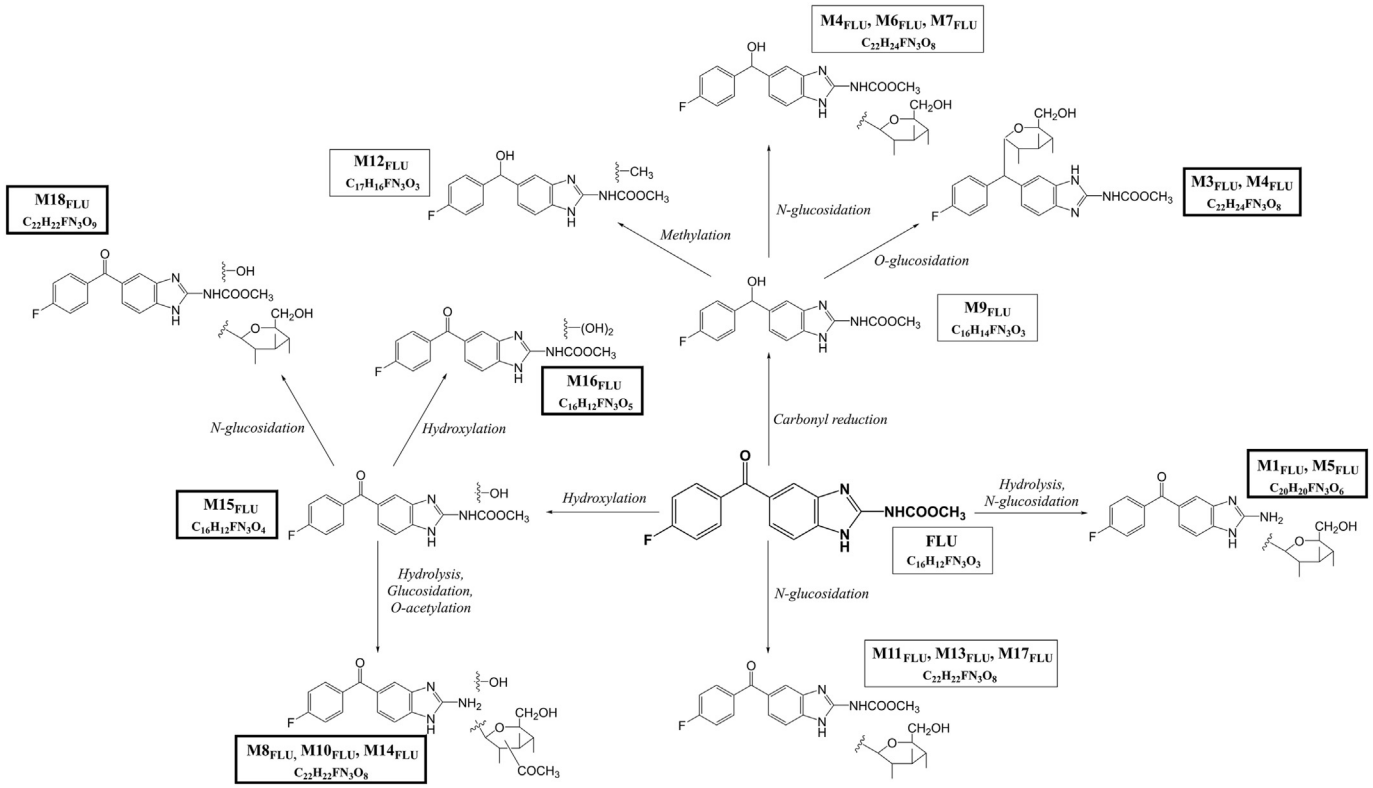

Fig. 2. Scheme of metabolic pathways of FLU in harebell cells *Campanula rotundifolia*. FLU metabolites that have not been found in other species are highlighted in bold rectangles.

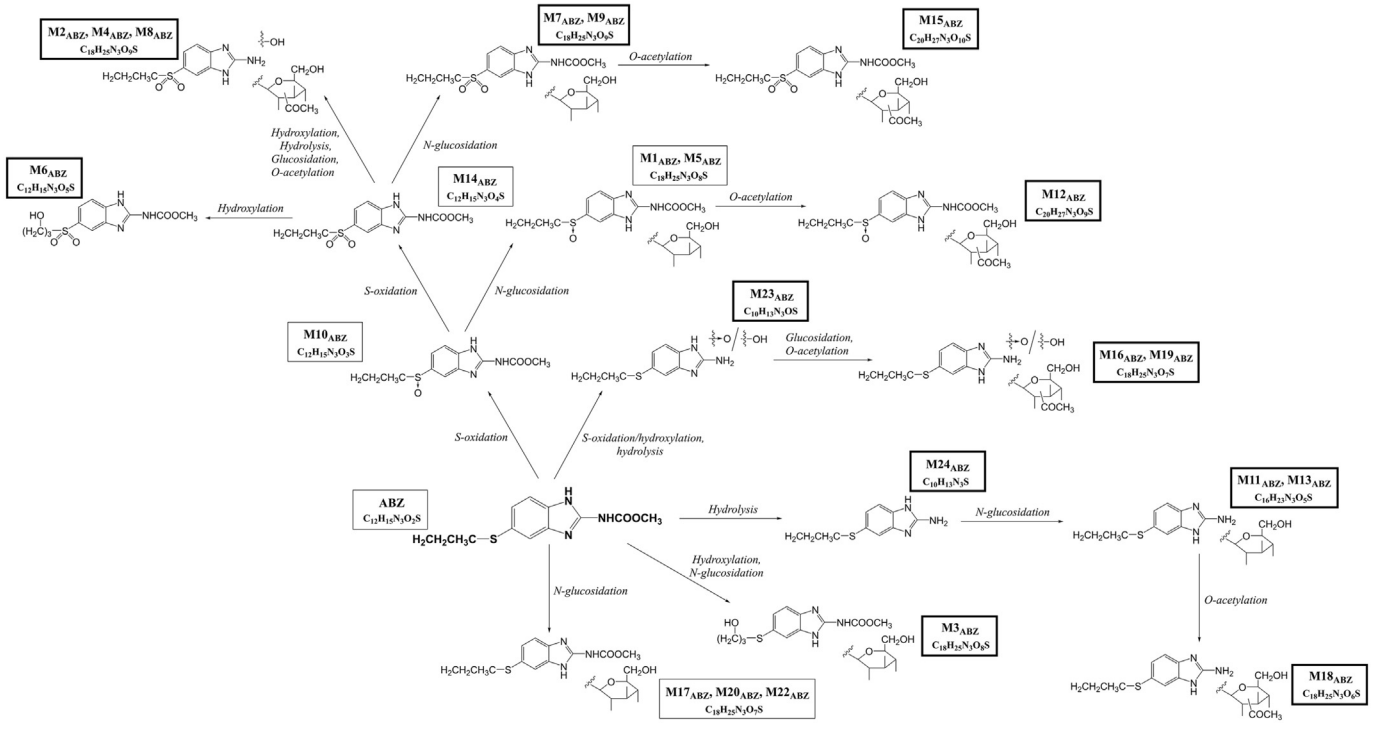

Fig. 3. Scheme of metabolic pathways of ABZ in harebell cells *Campanula rotundifolia*. ABZ metabolites that have not been found in other species are highlighted in bold rectangles.

Some glucosides of $M15_{FLU}$ metabolites were consequently acetylated, leading to the formation of $M8_{FLU}$ and $M10_{FLU}$ with the characteristic NL $\Delta m/z$ 220 (*O*-acetyl-glucoside).

Overall, the harebell cells were shown to form 18 metabolites of FLU. The scheme of proposed metabolic pathways is presented in Fig. 2.

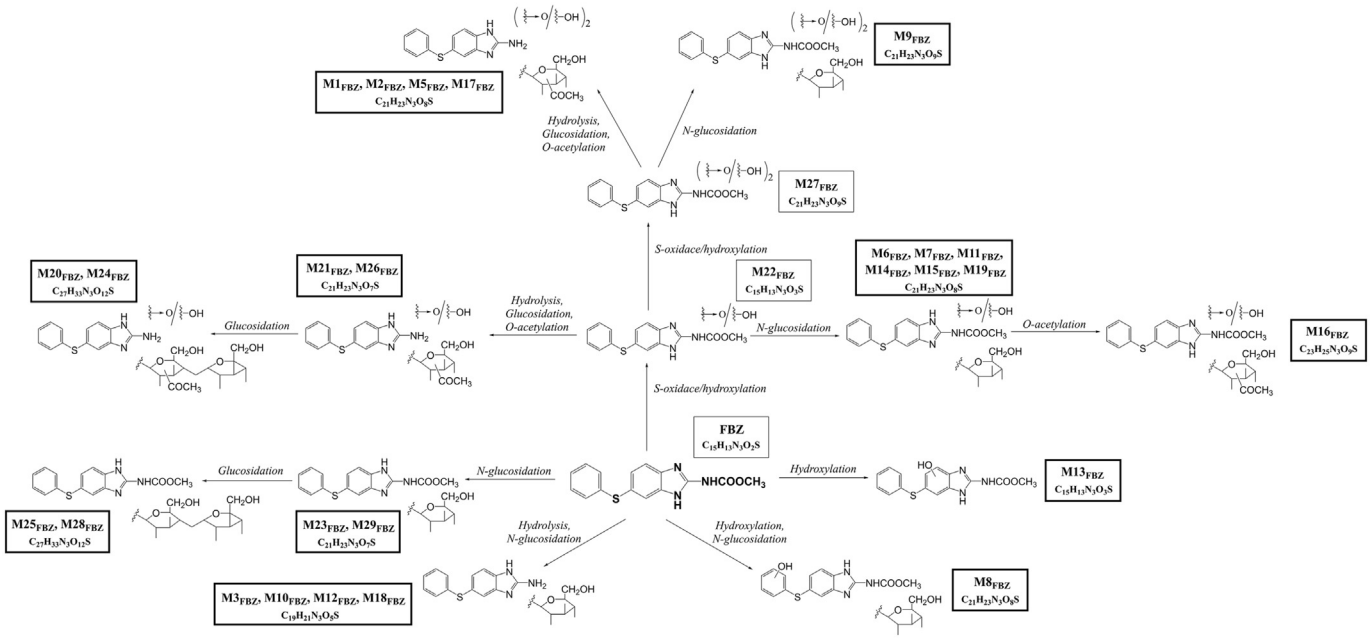

Fig. 4. Scheme of metabolic pathways of FBZ in harebell cells *Campanula rotundifolia*. FBZ metabolites that have not been found in other species are highlighted in bold rectangles.

Table 1
List of main peaks for FLU biotransformation samples detected by UHPLC-MS/MS with their retention times, theoretical values of $[M + H]^+$ ions in ESI positive-ion mode, elemental composition, product ions, and description of present metabolites.

t_R [min]	Theoretical *m/z* values of $[M + H]^+$ ions	Elemental composition	Description of metabolite formation		Product ions of $[M + H]^+$, *m/z*	Metabolite designation	Relative peak area [%]
			Phase I	Phase II			
2.65	418.1409	$C_{20}H_{20}FN_3O_6$	Hydrolysis	*N*-glucosidation	256, 123	$M1_{FLU}$	0.01
2.71	478.1620	$C_{22}H_{24}FN_3O_8$	Carbonyl reduction	Glucosidation	298, 266	$M2_{FLU}$	1.53
2.96	478.1620	$C_{22}H_{24}FN_3O_8$	Carbonyl reduction	Glucosidation	298, 266	$M3_{FLU}$	0.03
3.1	478.1620	$C_{22}H_{24}FN_3O_8$	Carbonyl reduction	*N*-glucosidation	316, 284	$M4_{FLU}$	0.37
3.13	418.1409	$C_{20}H_{20}FN_3O_6$	Hydrolysis	*N*-glucosidation	256	$M5_{FLU}$	<0.01
3.21	478.1620	$C_{22}H_{24}FN_3O_8$	Carbonyl reduction	*N*-glucosidation	316, 284	$M6_{FLU}$	0.02
3.6	478.1620	$C_{22}H_{24}FN_3O_8$	Carbonyl reduction	*N*-glucosidation	316, 284	$M7_{FLU}$	0.01
3.85	476.1464	$C_{22}H_{22}FN_3O_8$	Hydrolysis, hydroxylation	Glucosidation, *O*-acetylation	256	$M8_{FLU}$	0.01
3.91	316.1092	$C_{16}H_{14}FN_3O_3$	Carbonyl reduction	–	284, 238	$M9_{FLU}$	4.81
4.07	476.1464	$C_{22}H_{22}FN_3O_8$	Hydrolysis, hydroxylation	Glucosidation, *O*-acetylation	256	$M10_{FLU}$	0.64
4.34	476.1464	$C_{22}H_{22}FN_3O_8$	–	*N*-glucosidation	314, 282, 123	$M11_{FLU}$	0.78
4.59	330.1248	$C_{17}H_{16}FN_3O_3$	Carbonyl reduction	Methylation	298, 174	$M12_{FLU}$	0.01
4.66	476.1464	$C_{22}H_{22}FN_3O_8$	–	*N*-glucosidation	314, 282, 123	$M13_{FLU}$	7.56
4.78	476.1464	$C_{22}H_{22}FN_3O_8$	Hydrolysis, hydroxylation	Glucosidation, *O*-acetylation	256	$M14_{FLU}$	<0.01
4.96	330.0885	$C_{16}H_{12}FN_3O_4$	Hydroxylation	–	298	$M15_{FLU}$	<0.01
5.04	346.0833	$C_{16}H_{12}FN_3O_5$	2*hydroxylation	–	314	$M16_{FLU}$	<0.01
5.15	476.1464	$C_{22}H_{22}FN_3O_8$	–	*N*-glucosidation	314, 282	$M17_{FLU}$	0.09
5.40	492.1428	$C_{22}H_{22}FN_3O_9$	Hydroxylation	*N*-glucosidation	330, 298	$M18_{FLU}$	<0.01
7.03	314.0935	$C_{16}H_{12}FN_3O_3$		–	282, 123	FLU (parent drug)	84.13

3.2.2. Albendazole

The S-oxidation (the main pathway of phase I biotransformation) and hydrolysis are two initial steps of ABZ metabolism leading to formation of ABZ sulfoxide ($M10_{ABZ}$) and hydrolyzed ABZ ($M24_{ABZ}$). $M10_{ABZ}$ was consequently converted via second S-oxidation to sulfone ($M14_{ABZ}$). MS/MS spectra contained typical NL of Δ*m/z* 32 (methanol) and Δ*m/z* 42 (propene) for $M10_{ABZ}$ and $M14_{ABZ}$. Hydroxylation and hydrolysis were other type of phase I reaction in ABZ biotransformation ($M6_{ABZ}$, $M23_{ABZ}$).

The main pathway of phase II biotransformation, *N*-glucosidation of various metabolites of phase I ABZ biotransformation occurred ($M1_{ABZ}$, $M3_{ABZ}$, $M5_{ABZ}$, $M7_{ABZ}$, $M9_{ABZ}$, $M11_{ABZ}$, $M13_{ABZ}$ $M17_{ABZ}$, $M20_{ABZ}$ and $M22_{ABZ}$). The presence of conjugation with UDP-glucose is characterized by the NLs of Δ*m/z* 162 for glucose, Δ*m/z* 32 for methanol, and Δ*m/z* 42 for propene. In addition, *O*-acetylation was observed in several metabolites ($M12_{ABZ}$ and $M15_{ABZ}$). Conjugation with *O*-acetyl-glucosides were found ($M2_{ABZ}$, $M4_{ABZ}$, $M8_{ABZ}$, $M16_{ABZ}$, $M19_{ABZ}$ and $M21_{ABZ}$). NL of Δ*m/z* 220 corresponds to *O*-acetyl-glucoside and Δ*m/z* 204 corresponds to *O*-acetyl-*N*-glucoside for metabolites with acetylation.

In total, 24 metabolites of ABZ were formed in harebell cells. The scheme of proposed metabolic pathways of ABZ is presented in Fig. 3.

Table 2
List of main peaks for ABZ biotransformation samples detected by UHPLC-MS/MS with their retention times, theoretical values of $[M + H]^+$ ions in ESI positive-ion mode, elemental composition, product ions, and description of present metabolites.

t_R [min]	Theoretical *m/z* values of $[M + H]^+$ ions	Elemental composition	Description of metabolite formation		Product ions of [M + H]+, *m/z*	Metabolite designation	Relative peak area [%]
			Phase I	Phase II			
1.52	444.1435	$C_{18}H_{25}N_3O_8S$	S-oxidation	*N*-glucosidation	282, 240, 208, 191, 159	$M1_{ABZ}$	0.70
1.62	460.1384	$C_{18}H_{25}N_3O_9S$	2*S-oxidation, hydrolysis, hydroxylation	Glucosidation, *O*-acetylation	240	$M2_{ABZ}$	0.06
1.76	444.1435	$C_{18}H_{25}N_3O_8S$	Hydroxylation	*N*-glucosidation	282, 250, 222	$M3_{ABZ}$	1.28
1.79	460.1384	$C_{18}H_{25}N_3O_9S$	2*S-oxidation, hydrolysis, hydroxylation	Glucosidation, *O*-acetylation	240, 198	$M4_{ABZ}$	0.03
1.91	444.1435	$C_{18}H_{25}N_3O_8S$	S-oxidation	*N*-glucosidation	282, 240, 208	$M5_{ABZ}$	0.95
1.92	314.0805	$C_{12}H_{15}N_3O_5S$	2*S-oxidation, hydroxylation	–	238, 159	$M6_{ABZ}$	0.30
2.15	460.1384	$C_{18}H_{25}N_3O_9S$	2*S-oxidation	*N*-glucosidation	298, 266, 224, 191, 159	$M7_{ABZ}$	0.32
2.36	460.1384	$C_{18}H_{25}N_3O_9S$	2*S-oxidation, hydrolysis, hydroxylation	Glucosidation, *O*-acetylation	240, 133	$M8_{ABZ}$	0.58
2.54	460.1384	$C_{18}H_{25}N_3O_9S$	2*S-oxidation	*N*-glucosidation	298, 266, 224, 191, 159	$M9_{ABZ}$	0.02
2.6	282.0907	$C_{12}H_{15}N_3O_3S$	S-oxidation	–	240, 208, 191,159	$M10_{ABZ}$	61.18
2.92	370.1431	$C_{16}H_{23}N_3O_5S$	Hydrolysis	*N*-glucosidation	208, 166	$M11_{ABZ}$	3.26
3.21	486.1541	$C_{20}H_{27}N_3O_9S$	S-oxidation	*N*-glucosidation, *O*-acetylation	282, 240	$M12_{ABZ}$	0.11
3.55	370.1431	$C_{16}H_{23}N_3O_5S$	Hydrolysis	*N*-glucosidation	208	$M13_{ABZ}$	<0.01
4.11	298.0856	$C_{12}H_{15}N_3O_4S$	2*S-oxidation	–	266, 224, 159	$M14_{ABZ}$	10.85
4.26	502.1490	$C_{20}H_{27}N_3O_{10}S$	2*S-oxidation	*N*-glucosidation, *O*-acetylation	298, 160	$M15_{ABZ}$	0.05
4.30	428.1486	$C_{18}H_{25}N_3O_7S$	+O, hydrolysis	Glucosidation, *O*-acetylation	208	$M16_{ABZ}$	0.51
4.46	428.1486	$C_{18}H_{25}N_3O_7S$	–	*N*-glucosidation	266, 234, 191	$M17_{ABZ}$	4.35
4.69	412.1537	$C_{18}H_{25}N_3O_6S$	Hydrolysis	*N*-glucosidation, *O*-acetylation	–	$M18_{ABZ}$	<0.01
4.78	428.1486	$C_{18}H_{25}N_3O_7S$	+O, hydrolysis,	Glucosidation, *O*-acetylation	208	$M19_{ABZ}$	0.10
4.89	428.1486	$C_{18}H_{25}N_3O_7S$	–	*N*-glucosidation	266, 234	$M20_{ABZ}$	4.36
5.27	428.1486	$C_{18}H_{25}N_3O_7S$	+O, hydrolysis,	Glucosidation, *O*-acetylation	208, 250	$M21_{ABZ}$	0.89
5.42	428.1486	$C_{18}H_{25}N_3O_7S$	–	*N*-glucosidation	266, 234	$M22_{ABZ}$	8.68
6.26	266.0958	$C_{12}H_{15}N_3O_2S$	–	–	234	ABZ	1.42
7.85	224.0850	$C_{10}H_{13}N_3OS$	+O, hydrolysis,	–	–	$M23_{ABZ}$	<0.01
9.80	208.0902	$C_{10}H_{13}N_3S$	Hydrolysis	–	–	$M24_{ABZ}$	<0.01

As the measured data does not allow for the distinguishing of S-oxidation and hydroxylation, the metabolites were recorded as –O.

3.2.3. Fenbendazole

In phase I, FBZ was biotransformed via S-oxidation (the main pathway of phase I biotransformation), hydroxylation and hydrolysis ($M13_{FBZ}$, $M22_{FBZ}$ and $M27_{FBZ}$) with the characteristic NL $\Delta m/z$ 32 (methanol) and $\Delta m/z$ 18 (H_2O) found only for $M13_{FBZ}$. As the measured data does not allow for the determination of S-oxidation and hydroxylation, the metabolites were recorded as –O.

In phase II, FBZ underwent *N*-glucosidation, leading to the formation of $M23_{FBZ}$ and $M29_{FBZ}$. In addition, the FBZ phase I metabolites were conjugated with UDP-glucose ($M6\text{-}9_{FBZ}$, $M11_{FBZ}$, $M14_{FBZ}$, $M15_{FBZ}$ and $M19_{FBZ}$), the typical characterized NLs, $\Delta m/z$ 162 for glucose and $\Delta m/z$ 32 for methanol. An *N*-glucoside of hydrolyzed FBZ ($M3_{FBZ}$, $M10_{FBZ}$, $M12_{FBZ}$ and $M18_{FBZ}$) was also found. *O*-acetylation, the next step in the FBZ biotransformation pathway ($M1_{FBZ}$, $M2_{FBZ}$, $M5_{FBZ}$, $M16_{FBZ}$, $M17_{FBZ}$, $M21_{FBZ}$ and $M26_{FBZ}$) showed the characteristic NL $\Delta m/z$ 220. In the harebell cells, two metabolites corresponding of hydrolysed $M22_{FBZ}$ ($M20_{FBZ}$, $M24_{FBZ}$) were further detected and provided fragment ions at *m/z* 462, *m/z* 242. The position of bound glucosylglucose (*O*- or *N*-) in these metabolites was not determined. In contrast to ABZ and FLU, two FBZ *O*-glucosyl-*N*-glucosides ($M25_{FBZ}$ and $M28_{FBZ}$) were also identified, thus is the main pathway of phase II biotransformation.

All in all, 29 metabolites of FBZ were identified in the harebell cells. Fig. 4 presents the scheme of the proposed metabolic pathways of FBZ.

4. Discussion

Obviously most veterinary drugs have been present in the environment for a long time, but only now are the resultant long and short term effects being recognized, e.g. the fate, persistence and impact of these substances still remain unclear. The environment is inundated with many veterinary drugs directly via the treatment of animals at pasture or indirectly through the application of manure and other waste materials to land or its seepage into water (Piotrowicz-Cieslak et al., 2012). Consequently, many veterinary drugs as well as other environmental contaminants enter plant organisms, clearly representing a potential danger to them.

The majority of studies regarding the phytotoxicity of veterinary drugs have been focused on veterinary antibiotics, with their toxicity in plants varying among plant species and types of antibiotic compounds. Nevertheless, particular compounds have been shown to possess significant phytotoxicity in certain plants ((Du and Liu, 2012) and (Kumar et al., 2012)). With regard to anthelmintics, no adverse effect from FLU and FBZ on the growth of duckweed *Lemna minor* has been observed (Wagil et al., 2015). In our study, ABZ, FBZ and FLU did not express significant acute toxicity on harebell cells.

Plants are able to uptake xenobiotics, including drugs, and detoxify them via biotransformation as a result of sophisticated detoxification systems which plants have evolved against potentially toxic chemicals: following the uptake, the compounds formed

Table 3
List of main peaks for FBZ biotransformation samples detected by UHPLC-MS/MS with their retention times, theoretical values of $[M + H]^+$ ions in ESI positive-ion mode, elemental composition, product ions, and description of present metabolites.

t_R [min]	Theoretical *m/z* values of $[M + H]^+$ ions	Elemental composition	Description of metabolite formation		Product ions of $[M + H]+$, *m/z*	Metabolite designation	Relative peak area [%]
			Phase I	Phase II			
2.05	478.1278	$C_{21}H_{23}N_3O_8S$	2*(+O), hydrolysis	Glucosidation, *O*-acetylation	258, 133	$M1_{FBZ}$	<0.01
2.24	478.1278	$C_{21}H_{23}N_3O_8S$	2*(+O), hydrolysis	Glucosidation, *O*-acetylation	258	$M2_{FBZ}$	0.17
2.57	404.1274	$C_{19}H_{21}N_3O_5S$	Hydrolysis	*N*-glucosidation	–	$M3_{FBZ}$	<0.01
2.62	478.1278	$C_{21}H_{23}N_3O_8S$	+O	*N*-glucosidation	316, 284, 299, 267, 239, 191, 159	$M4_{FBZ}$	0.77
2.79	478.1278	$C_{21}H_{23}N_3O_8S$	2*(+O), hydrolysis	Glucosidation, *O*-acetylation	258, 300	$M5_{FBZ}$	0.13
3.08	478.1278	$C_{21}H_{23}N_3O_8S$	+O	*N*-glucosidation	316, 284, 191	$M6_{FBZ}$	0.18
3.25	478.1278	$C_{21}H_{23}N_3O_8S$	+O	*N*-glucosidation	316, 284	$M7_{FBZ}$	4.13
3.42	478.1278	$C_{21}H_{23}N_3O_8S$	Hydroxylation	*N*-glucosidation	316, 284, 222, 192, 160	$M8_{FBZ}$	0.02
3.75	494.1227	$C_{21}H_{23}N_3O_9S$	2*S-oxidation	*N*-glucosidation	332, 300	$M9_{FBZ}$	<0.01
3.83	404.1274	$C_{19}H_{21}N_3O_5S$	Hydrolysis	*N*-glucosidation	242	$M10_{FBZ}$	0.08
3.91	478.1278	$C_{21}H_{23}N_3O_8S$	+O	*N*-glucosidation,	284	$M11_{FBZ}$	0.38
4.13	404.1274	$C_{19}H_{21}N_3O_5S$	Hydrolysis	*N*-glucosidation	242, 133	$M12_{FBZ}$	6.79
4.29	316.0750	$C_{15}H_{13}N_3O_3S$	Hydroxylation	–	266, 207, 191, 175, 159, 131	$M13_{FBZ}$	2.32
4.36	478.1278	$C_{21}H_{23}N_3O_8S$	+O	*N*-glucosidation	316, 284, 192, 160, 159	$M14_{FBZ}$	0.62
4.42	478.1278	$C_{21}H_{23}N_3O_8S$	+O	*N*-glucosidation	316, 284, 191	$M15_{FBZ}$	0.02
4.61	520.1384	$C_{23}H_{25}N_3O_9S$	+O	*N*-glucosidation, *O*-acetylation	316, 299, 284, 207, 191, 159	$M16_{FBZ}$	0.64
4.77	478.1278	$C_{21}H_{23}N_3O_8S$	2*(+O), hydrolysis	Glucosidation, *O*-acetylation	258	$M17_{FBZ}$	0.03
4.8	404.1274	$C_{19}H_{21}N_3O_5S$	Hydrolysis	*N*-glucosidation	242	$M18_{FBZ}$	0.85
4.87	478.1278	$C_{21}H_{23}N_3O_8S$	+O	*N*-glucosidation	316, 284, 160	$M19_{FBZ}$	0.01
4.96	624.1842	$C_{27}H_{33}N_3O_{12}S$	+O, hydrolysis	2*glucosidation, O-acetylation	462, 368, 242	$M20_{FBZ}$	0.01
5.57	462.1329	$C_{21}H_{23}N_3O_7S$	+O, hydrolysis	Glucosidation, *O*-acetylation	320, 242	$M21_{FBZ}$	1.78
5.62	316.0750	$C_{15}H_{13}N_3O_3S$	+O	–	284, 238, 191, 160	$M22_{FBZ}$	<0.01
5.65	462.1329	$C_{21}H_{23}N_3O_7S$	–	*N*-glucosidation	300, 268, 159	$M23_{FBZ}$	<0.01
5.76	624.1825	$C_{27}H_{33}N_3O_{12}S$	+O, hydrolysis	2*glucosidation, O-acetylation	462, 342, 242	$M24_{FBZ}$	0.26
5.85	624.1839	$C_{27}H_{33}N_3O_{12}S$	–	2*glucosidation,	300, 268	$M25_{FBZ}$	0.06
5.96	462.1329	$C_{21}H_{23}N_3O_7S$	+O, hydrolysis	Glucosidation, *O*-acetylation	242	$M26_{FBZ}$	2.86
6.27	332.0699	$C_{21}H_{23}N_3O_9S$	2*(+O)	–	300, 159	$M27_{FBZ}$	0.02
6.36	624.1838	$C_{27}H_{33}N_3O_{12}S$	–	2*glucosidation,	300, 268	$M28_{FBZ}$	42.45
6.86	462.1329	$C_{21}H_{23}N_3O_7S$	–	*N*-glucosidation	300, 268, 159	$M29_{FBZ}$	19.16
8.53	300.0801	$C_{15}H_{13}N_3O_2S$	–	–	268, 159, 131	FBZ	16.25

As the measured data does not allow for the distinguishing of S-oxidation and hydroxylation, the metabolites were recorded as –O.

in biotransformation are activated so that certain functional groups can conjugate hydrophilic molecules. The resulting conjugates are recognized by tonoplast transporters and sequestered into the vacuoles or transferred to the apoplast (Puglisi et al., 2013). Xenobiotic-metabolizing enzymes facilitate the detoxification of potentially harmful xenobiotics, with this enzyme activity being crucial for the neutralization of the effects of xenobiotics both in the exposed organism as well as in the environment on the whole. Generally, the parent substance and the metabolite or conjugate have different physico-chemical properties which differ in both biological activity (including toxicity) and behavior in organisms. Significant inter-species differences in the occurrence, affinity and activity of xenobiotic-metabolizing enzymes determine dissimilarities regarding the biotransformation pathways of each xenobiotic in an individual species.

In a previous study of ours, the biotransformation of ABZ and FLU was studied *in vitro* in the common reed (*Phragmites australis*), a wetland species often used in phytoremediation studies. Our results showed that reed cells were able to metabolize both of these anthelmintics: 5 metabolites of FLU and 10 metabolites of ABZ were identified (Podlipna et al., 2013). In our present study, harebell was chosen as an experimental plant because it represents a common meadow species which is likely to come in contact with anthelmintics in grazing pastures. In addition to FLU and ABZ, FBZ was also included in the study, as the negative impact of FBZ on invertebrates has already been reported (Oh et al., 2006) (Park et al., 2009). Moreover, the relative peak area of each parent drug and its metabolites in harebell cells have been measured to obtain more complex information about benzimidazoles biotransformation. Nevertheless, in comparing the existing studies of the biotransformation of anthelmintics in reed and in harebell cells, it must be taken account that the detection and identification of metabolites were performed in different types of mass spectrometers with differing resolving power.

In harebell, FLU, ABZ and FBZ were transformed into 18, 24 and 29 metabolites, respectively. After 24-h incubation, approx. 98%, 84% and 16% of parent ABZ, FBZ and FLU were transformed into metabolites. These results show great differences in the ability of plant cells to metabolize individual benzimidazoles. While almost all the ABZ was metabolized, only 16% of the FLU was transformed after 24-h incubation.

ABZ.SO, ABZ.SO_2 and ABZ-*N*-glucosides represented the main ABZ metabolites in harebells. Interestingly, some of ABZ metabolites (e.g. ABZ-glucosylglucosides, ABZ-xylosylglucoside) observed

in reeds were not found in harebell. Conversely, harebell cells metabolized ABZ via the second S-oxidation, hydrolysis and hydroxylation, however reed cells did not. As the formation of anthelmintically inactive ABZ.SO_2 and hydrolyzed ABZ denotes ABZ deactivation, harebell seems to have a better potency for ABZ detoxification than does the reed.

The main metabolites of FLU were FLU with reduced carbonyl group and FLU-*N*-glucosides. FLU hydrolysis and hydroxylation, which characterized the other biotransformation ways of FLU in harebell, were not observed in the reed. These findings serve to underscore the great inter-species differences in the drug metabolism among plants.

Prior to the present work, the metabolism of FBZ had not been studied yet in plants. Harebell cells were able metabolize FBZ via two-step sulfoxidation or hydroxylation and hydrolysis followed by *N*-glucosidation and *O*-acetylation. *N*-glucosides were the main FBZ metabolites. Similarly to ABZ and FLU, most of the metabolites of FBZ can be considered deactivation products. Nonetheless, the consumption of harebells with accumulated anthelmintics and their metabolites by herbivores and leaf-eating invertebrates may present a clear risk of the animals being exposed to anthelmintics. In addition, the influence of anthelmintics and their biotransformation on plant signaling and protective processes cannot be excluded. For these reasons, after treatment with anthelmintics, animals should not be grazed on pastures (especially on those with a high ecological value) until such time as the drugs are no longer in their system.

5. Conclusions

Benzimidazole anthelmintics ABZ, FLU and FBZ were not found to be toxic for harebell cells; nevertheless, a possible influence of chronic exposure cannot be excluded. Harebell cells transformed ABZ, FLU and FBZ into 24, 18 and 29 metabolites, respectively. S-oxidation, hydroxylation, carbonyl reduction and hydrolysis comprised the phase I biotransformation of these anthelmintics. In phase II, many various glucosides, acetylglucosides and glucosylglucosides were formed in the harebell cells. Most of these metabolites can be considered deactivation products, but a number of them remain biologically active. Moreover, a substantial portion of the metabolites were instable and could be easily decomposed back to the parent anthelmintic. In any event, the grazing of treated animals in pastures with valuable ecosystems should be limited.

Acknowledgement

This project was supported by the Czech Science Foundation (GA ČR, grant No. 15-05325S) and by Charles University in Prague (research project SVV 260 294). We thank Daniel Paul Sampey, MDA for English revision.

References

Arnold, K.E., Boxall, A.B.A., Brown, A.R., Cuthbert, R.J., Gaw, S., Hutchinson, T.H., Jobling, S., Madden, J.C., Metcalfe, C.D., Naidoo, V., Shore, R.F., Smits, J.E., Taggart, M.A., Thompson, H.M., 2013. Assessing the exposure risk and impacts of pharmaceuticals in the environment on individuals and ecosystems. Biol. Lett. 9.

Boxall, A., Long, C., 2005. Veterinary medicines and the environment. Environ. Toxicol. Chem. 24, 759–760.

Boxall, A.B.A., Kolpin, D.W., Halling-Sorensen, B., Tolls, J., 2003. Are veterinary medicines causing environmental risks? Environ. Sci. Technol. 37, 286A–294A.

Boxall, A.B.A., Rudd, M.A., Brooks, B.W., Caldwell, D.J., Choi, K., Hickmann, S., Innes, E., Ostapyk, K., Staveley, J.P., Verslycke, T., Ankley, G.T., Beazley, K.F., Belanger, S.E., Berninger, J.P., Carriquiriborde, P., Coors, A., DeLeo, P.C., Dyer, S.D., Ericson, J.F., Gagne, F., Giesy, J.P., Gouin, T., Hallstrom, L., Karlsson, M.V., Larsson, D.G.J., Lazorchak, J.M., Mastrocco, F., McLaughlin, A., McMaster, M.E., Meyerhoff, R.D., Moore, R., Parrott, J.L., Snape, J.R., Murray-Smith, R., Servos, M.R., Sibley, P.K., Straub, J.O., Szabo, N.D., Topp, E., Tetreault, G.R., Trudeau, V.L., Van Der Kraak, G., 2012. Pharmaceuticals and personal care products in the environment: what are the big questions? Environ. Health Perspect. 120, 1221–1229.

Cummins, I., Dixon, D.P., Freitag-Pohl, S., Skipsey, M., Edwards, R., 2011. Multiple roles for plant glutathione transferases in xenobiotic detoxification. Drug Metab. Rev. 43, 266–280.

Doran, P.M., 2009. Application of plant tissue cultures in phytoremediation research: incentives and limitations. Biotechnol. Bioeng. 103, 60–76.

Du, L.F., Liu, W.K., 2012. Occurrence, fate, and ecotoxicity of antibiotics in agro-ecosystems. A review. Agron. Sustain Dev. 32, 309–327.

Floate, K.D., Wardhaugh, K.G., Boxall, A.B.A., Sherratt, T.N., 2005. Fecal residues of veterinary parasiticides: nontarget effects in the pasture environment. Annu. Rev. Entomol. 153–179.

Gao, Y.H., Sun, Z.J., Sun, X.S., Sun, Y., Shi, W.Y., 2007. Toxic effects of albendazole on adenosine triphosphatase activity and ultrastructure in Eisenia fetida. Ecotoxicol. Environ. Saf. 67, 378–384.

Gonzalez-Mendoza, D., 2007. Enzymatic complex cytochrome P450 in plants. Rev. Int. De. Contam. Ambient. 23, 177–183.

Harhay, M.O., Horton, J., Olliaro, P.L., 2010. Epidemiology and control of human gastrointestinal parasites in children. Expert Rev. Anti-Infective Ther. 8, 219–234.

Holčapek, M., Kolářová, L., Nobilis, M., 2008. High-performance liquid chromatography-tandem mass spectrometry in the identification and determination of phase I and phase II drug metabolites. Anal. Bioanal. Chem. 391, 59–78.

Horvat, A.J.M., Petrovic, M., Babic, S., Pavlovic, D.M., Asperger, D., Pelko, S., Mance, A.D., Kastelan-Macan, M., 2012. Analysis, occurrence and fate of anthelmintics and their transformation products in the environment. Trac-Trends Anal. Chem. 31, 61–84.

Kumar, R.R., Lee, J.T., Cho, J.Y., 2012. Fate, occurrence, and toxicity of veterinary antibiotics in environment. J. Korean Soc. Appl. Bi 55, 701–709.

Murashige, T., Skoog, F., 1962. A revised medium for rapid growth and bio assays with tobacco tissue cultures. Physiol. Plant. 15, 473–497.

Oh, S.J., Park, J., Lee, M.J., Park, S.Y., Lee, J.H., Choi, K., 2006. Ecological hazard assessment of major veterinary benzimidazoles: acute and chronic toxicities to aquatic microbes and invertebrates. Environ. Toxicol. Chem. 25, 2221–2226.

Park, K., Bang, H.W., Park, J., Kwak, I.S., 2009. Ecotoxicological multilevel-evaluation of the effects of fenbendazole exposure to Chironomus riparius larvae. Chemosphere 77, 359–367.

Piotrowicz-Cieslak, A.I., Adomas, B., Nalecz-Jawecki, G., 2012. Phytotoxicity of sulfonamide soil pollutants to legume plant species. Fresenius Environ. Bull. 21, 1310–1314.

Podlipna, R., Fialova, Z., Vanek, T., 2008. Toxic effect of nitroesters on plant tissue cultures. Plant Cell Tissue Organ Cult. 94, 305–311.

Podlipna, R., Skalova, L., Seidlova, H., Szotakova, B., Kubicek, V., Stuchlikova, L., Jirasko, R., Vanek, T., Vokral, I., 2013. Biotransformation of benzimidazole anthelmintics in reed (Phragmites australis) as a potential tool for their detoxification in environment. Bioresour. Technol. 144, 216–224.

Podlipna, R., Pospsilova, B., Vanek, T., 2015. Biodegradation of 2,4-dinitrotoluene by different plant species. Ecotoxicol. Environ. Saf. 112, 54–59.

Puglisi, I., Lo Cicero, L., Lo Piero, A.R., 2013. The glutathione S-transferase gene superfamily: an in silico approach to study the post translational regulation. Biodegradation 24, 471–485.

Sutherland, I.A., Leathwick, D.M., 2011. Anthelmintic resistance in nematode parasites of cattle: a global issue? Trends Parasitol. 27, 176–181.

Verkleij, J.A.C., Golan-Goldhirsh, A., Antosiewisz, D.M., Schwitzguebel, J.P., Schroder, P., 2009. Dualities in plant tolerance to pollutants and their uptake and translocation to the upper plant parts. Environ. Exp. Bot. 67, 10–22.

Vokřál, I., Bártíková, H., Prchal, L., Stuchlíková, L., Skálová, L., Szotáková, B., Lamka, J., Várady, M., Kubíček, V., 2012. The metabolism of flubendazole and the activities of selected biotransformation enzymes in *Haemonchus controtus* strains susceptible and resistant to anthelmintics. Parasitology 139, 1309–1316.

Wagil, M., Bialk-Bielinska, A., Puckowski, A., Wychodnik, K., Maszkowska, J., Mulkiewicz, E., Kumirska, J., Stepnowski, P., Stolte, S., 2015. Toxicity of anthelmintic drugs (fenbendazole and flubendazole) to aquatic organisms. Environ. Sci. Pollut. R. 22, 2566–2573.